Characterization of Silane Layers on Modified Stainless Steel Surfaces and Related Stainless Steel-Plastic Hybrids

Mari Honkanen[a,*], Maija Hoikkanen[b], Minnamari Vippola[a], Jyrki Vuorinen[b], and Toivo Lepistö[a]

Petri Jussila[c], Harri Ali-Löytty[c], Markus Lampimäki[c], and Mika Valden[c]

[a] Laboratory of Materials Characterization and [b] Laboratory of Plastics and Elastomer Technology, Department of Materials Science, Tampere University of Technology, P.O.B. 589, FIN-33101 Tampere, Finland

[c] Surface Science Laboratory, Tampere University of Technology, P.O.B. 692, FIN-33101 Tampere, Finland

[*]Corresponding author: Mari Honkanen, e-mail address: mari.honkanen@tut.fi, postal address: Department of Materials Science, Tampere University of Technology, P.O.B. 589, FIN-33101 Tampere, Finland, telephone: +358408490133, fax: +358331152330

Graphical abstract:

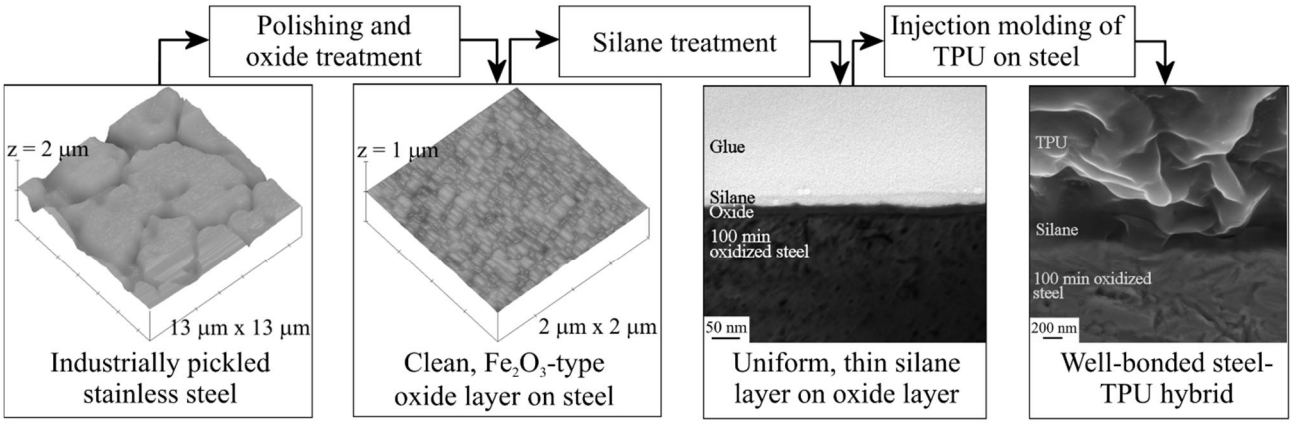

Silane bonding to cleaned, industrially pickled stainless steel is poor so, modification of steel surface is needed to achieve well-bonded steel-TPU hybrids

Highlights:

- AFM, FESEM, and TEM are useful to obtain quantitative information on silane layers
- Information on layers can be linked to adhesion and failure type of hybrids
- Controlled Fe_2O_3-type surface is needed to achieve uniform silane layer
- Silane layer on controlled oxide layer has more N-species to react with plastic

Abstract

The aim of this work was to characterize silane layers on the modified stainless steel surfaces and relate it to the adhesion in the injection-molded thermoplastic urethane-stainless steel hybrids. The silane layers were characterized with scanning electron microscope and transmission electron microscope, allowing the direct quantization of silane layer thickness and its variation. The surface topographies were characterized with atomic force microscope and chemical analyses were performed with X-ray photoelectron spectroscopy. The mechanical strength of the respective stainless steel-thermoplastic urethane hybrids was determined by peel test. Polishing and oxidation treatment of the steel surface improved the silane layer uniformity compared to the industrially pickled surface and increased the adhesion strength of the hybrids, resulting mainly cohesive failure in TPU. XPS analysis indicated that the improved silane bonding to the modified steel surface was due to clean Fe_2O_3-type surface oxide and stronger interaction with TPU was due to more amino species on the silane layer surface compared to the cleaned, industrially pickled surface. Silane layer thickness affected failure type of the hybrids, with a thick silane layer the hybrids failed mainly in the silane layer and with a thinner layer cohesively in plastic.

Keywords: metal-plastic hybrids; silane; AFM; TEM; SEM; XPS

1. INTRODUCTION

Metal-plastic hybrids are innovative products combining dissimilar materials and their properties in the same component. They can offer benefits which are not achieved with individual material alone e.g.: savings in weight, part reduction, better dimensional stability, and manufacturing multi-functional components in a few processing steps. Metal-plastic hybrids can replace metal structures for example in cars, appliances, laptops, and sporting goods. However, joining of materials is very challenging. This is because of the fact that two physically and chemically very different materials are combined together. Bonds between them can be achieved by chemical or physical bonding mechanisms or by mechanical interlocking like perforating metal insert and over-molding polymer on it, which is the mainly used method in industrial applications. However, in many applications like in electronic components, planar inserts without perforation are needed, but a detailed knowledge of the adhesion between metal and plastic is still lacking. In earlier study [1], the results about silicon-based coupling agents to promote chemical adhesion between planar metal insert and plastic in the injection-molded metal-plastic hybrid structures were promising.

Silanes are the most commonly used coupling agents to bond organic and inorganic materials. Widely used functional organosilanes have typically a structure:

$$X_3Si(CH_2)_n\text{-}Y \qquad (1)$$

Where X is a hydrolyzable group (e.g. methoxy, ethoxy, or acetoxy) and Y is an organofunctional group (e.g. amino, methacryloxy, or epoxy). The value of n is typically 3 [2-6].

Usually, silane treatment of the substrates consists of three steps: hydrolysis of silane, silanization of the substrate, and thermal curing of the silanized substrate [5]. Silane solutions are usually very dilute (0.01-2%) because in a dilute solution, reactive hydrolyzed molecules do not react with each other [4]. When a substrate is immersed into the hydrolyzed silane solution, silanol groups (SiOH) adsorb spontaneously onto the substrate through hydrogen bonds. During drying and curing processes, two condensation reactions occur in the silane/metal interface: SiOH groups and metal hydroxyls (MeOH) form a stable and covalent oxane bond (MeOSi) and silanol groups react with each other on the metal surface, resulting a siloxane network structure (SiOSi). Water evaporates during both processes [5-7]. SiOSi bonds can form already at room temperature, while SiOMe bonds need elevated temperature [8]. Silane bonding to polymer is complex and it is dominated by the organofunctionality of silane and polymer characteristics [4].

Thickness of the coupling agent layer is an important factor in the adhesion phenomenon. With too thin or thick layers, adhesion will suffer [3, 9]. The thick siloxane layer can contain a chemical layer and a physical absorbed layer and a weak interface layer can decrease the adhesive strength. Thicker films can also become brittle [10]. However, the optimum thickness depends on bonded materials [3]. A substrate surface influences also silane layer formation. A rough surface may disturb the order of the first silane layer preventing the formation of the second [4]. Thus, smooth surfaces are the best substrates for silane bonding. In earlier study [1], silane bonding to the industrially pickled stainless steel surface was very poor while, a controlled oxide layer, mainly of the types Fe_2O_3 and Cr_2O_3 [11], improves significantly silane adhesion on the stainless steel surface [1]. Susac et al. [12] and Kim et al. [13] also noticed similar behavior with organosilane - aluminum alloy combinations.

Silane layers on metals are usually characterized by: XPS, infra-red spectroscopy (IR), and ellipsometry to determine layer thicknesses, elemental compositions, and chemical states. P. Jussila *et al.* studied adsorption of APS (3-aminopropyltrimethoxysilane) on stainless steel surface by XPS, focusing on the formation of SiOSi, SiOMe, and –OH type bonds at the oxide/silane interface [8]. G. Li *et al*. [10] studied the chemical structure of g-GPS (g-glycidoxypropyltrimethoxysilane) on the low carbon steel surfaces and W. Yuan *et al*. [14] g-APS (g-aminopropyltriethoxysilane) on the zinc surface by reflection-absorption IR. They detected absorption bands like: SiOH, SiOSi, and NH_2. W. Yuan *et al*. [14] detected with XPS that the amount of silicon in the g-APS layer (from the solution concentration of 1 vol%) on the zinc surface was 4, 7, and 7 at% depending on the solution pH 4.5, 8, and 10.3, respectively. While G. Li et al. [10] studied the elemental distribution of the g-GPS layer (from the solution concentration of 10 vol%) with an energy dispersive X-ray spectrometer (EDS) and they observed that the amount of silicon in the layer was 12, 76, and 31 at% depending on the curing temperature 100, 150, and 200°C, respectively. C. Le Pen *et al.* [15] studied BTSE (bis-1,2-(triethoxysilyl)ethane) on aluminum by e.g. spectroscopic ellipsometer to determine the layer thickness as the function of BTSE solution concentration. They noticed a linear relation between the layer thickness (around 100-450 nm) and the solution concentration (2-10 %). Previous methods give numerical values about silane layers but it would be very important also to visualize them. However, for example cross-sectional electron microscopy studies about various silane layers on metal surfaces are almost lacking. To the best of our knowledge, only few articles about the electron microscopy of silanes on the metal surfaces have been published. A. Franquet *et al.* [16] and De Graeve *et al.* [17] studied the cross-sections of BTSE on aluminum with electron microscope. BTSE is non-functional silane and therefore usually used for the corrosion protection of the metal surface not as an adhesion promoter in organic-inorganic applications.

The aim of this work was to characterize silane layers on the modified stainless steel surfaces and relate it to the adhesion in the injection-molded thermoplastic urethane-stainless steel hybrids. Prior to silanization, the steel surfaces were modified by polishing and oxidation treatments (in air at 350 °C for 5 or 100 minutes) and its effect on the formed silane layers compared to the cleaned, industrially pickled steel surface was studied. Topographies of the steel surfaces and silane layers on them were studied with AFM. Chemical analysis of the surfaces before and after silanization was performed with XPS. Thickness and uniformity of the silane layers were studied with SEM and TEM. The adhesion strength of the hybrids was measured with peel tests and peeled sample surfaces were studied with FESEM and AFM.

2. MATERIAL AND METHODS

2.1. Materials

Insert material was stainless steel AISI 304 from Outokumpu (Finland). The as-received steel plate was cold-rolled, heat-treated, pickled, and skin-passed. The inserts, 100 mm x 12 mm x 0.5 mm, were laser-cut from the steel plate by JaloteräsStudio (Finland). The composition of AISI 304, based on the material certificate received by Outokumpu, is presented in Tab. 1.

Table 1. Composition [%] of AISI 304, based on material certificate received from Outokumpu.

C	Si	Mn	P	S	Cr	Ni	Fe
0.050	0.530	1.700	0.030	0.001	18.200	8.200	bal

Coupling agent used was amino-functional N-(b-aminoethyl)-g-aminopropyltrimethoxysilane (g-AEAPS, commercially available as Dow Corning Z-6020, Dow Corning, USA) with chemical structure:

$$H_2NC_2H_4NHC_3H_6\text{-}Si(OCH_3)_3 \quad (5)$$

Polymer in the injection-molded steel-silane-plastic hybrids was thermoplastic urethane (TPU, commercially available as Estane GP 85 AE nat, Lubrizol Advanced Materials Inc., USA).

2.2. Manufacturing process of steel-TPU hybrids

The manufacturing process of the metal-plastic hybrids consists of three steps: the surface modifications of the steel insert, the silane treatment of the steel insert, and the injection molding of plastic onto steel insert. Below, the different steps are described more carefully.

Three surface modifications were used for the industrially pickled surface of AISI 304: (1) washing with acetone and ethanol in an ultrasonic cleaner for 6 minutes, (2) electrolytic polishing and oxidation treatment in air at 350 °C for 5 minutes, and (3) electrolytic polishing and oxidation treatment in air at 350 °C for 100 minutes. Prior to oxidation treatments, industrial electrolytic polishing by JaloteräsStudio was carried out to achieve a clean and smooth surface for further oxidation treatments. According to earlier studies [1], a controlled oxide layer on steel improves bonding between steel and silane and hence steel and plastic. In the metal-plastic hybrid structure, the best peel strength values were achieved with electrolytically polished and 5 or 100 minutes oxidized (in air at 350 °C) steel inserts. Therefore in this study, the electrolytically polished stainless steel inserts were oxidized in air at 350 °C for 5 or 100 minutes to achieve a controlled oxide layer, consisting of mainly Fe_2O_3 and Cr_2O_3. During 5 minutes oxidation treatment, single

oxide islands formed on the base oxide layer and after 100 minutes, the islands have combined to form a uniform layer [11].

Various silane treatment parameters have been tested in the previous study [9] and the parameters in this study were based on those results. Solution concentration was 0.5 vol% at natural pH 9-10 and deionized water was used as the solvent. The solution was stirred for 1 hour for hydrolyzation, and the inserts were then dipped in solution for 5 minutes. During dipping, approximately 65% of the insert was in the solution leaving thus 35% in non-treated condition. Curing, to achieve covalent SiOMe bonds [8], was performed in air at 110 °C for 10 minutes in the angle of 30 ° from the horizontal plane to allow excess silane solution to flow to the bottom of the insert.

TPU was injection-molded onto the silanized steel inserts. The TPU-steel hybrid parts were processed with an electric injection molding machine (Fanuc Roboshot αC30, Japan). Molding parameters were similar than in previous study [1]. The finished hybrid component had 0.5 mm thick stainless steel insert and 2 mm thick TPU layer and the silane layer between them.

2.3. Characterization of silanized steel inserts and injection-molded steel-TPU hybrids

2.3.1. AFM

Topographies of the various steel inserts before and after silane treatment and also after the peel tests were studied with AFM (Nanoscope E AFM/STM, Digital Instruments Inc., USA). A pyramidal probe and a 200 mm long triangular cantilever made of silicon nitride were used with a spring constant of 0.12 N/m. Contact and constant force modes were used. Surface roughness values (R_a) of the samples were calculated from AFM images with the support of software.

2.3.2. XPS

Chemical analysis of sample surfaces was performed by XPS (XSAM 800, Kratos Analytical, UK) employing non-monochromated Al *Kα* radiation (photon energy = 1486.6 eV). The cleaned, industrially pickled surface and polished, 100 min oxidized steel surface were investigated before and after silanization. Spectra were recorded at normal emission geometry using fixed retarding ratio mode for survey spectra (retarding ratio = 20) and fixed analyzer transmission mode for narrow scan spectra (pass energy = 38.0 eV). Base pressure during the measurements was below 1×10^{-8} mbar.

The chemical states of elements were determined from XPS spectra by least-squares fitting of Gaussian-Lorentzian lineshapes with a Shirley type background to the main photoelectron peaks. The analysis was carried out using CasaXPS software (version 2.3.13) [18]. All binding energy values were referenced to the Fe $2p_{3/2}$ peak (707.0 eV for metallic Fe and 711.2 eV for Fe_2O_3) [19], because the commonly used C 1*s* peak may shift as much as 1 eV between silanes and carbonous impurities [8].

2.3.3. TEM and SEM

After the silane treatment, silane layers were studied with TEM (Jeol JEM 2010, Jeol, Japan) operated at an accelerating voltage of 200 kV and equipped with energy dispersive X-ray spectrometer (EDS, Noran Vantage Si(Li) detector, Thermo Scientific, USA). To study the composition of the silane layer, the layer was carefully scraped with surgical blade from the silanized steel surface and the layer was set on a copper grid with holey carbon film. The cross-sections of the silane layers were also characterized with TEM to measure layer thicknesses and to study the steel/silane interfaces. For the cross-sectional TEM studies, the small pieces of the silanized steels were cut to size ~1.5 mm x 1 mm x 0.5 mm. The pieces were attached to the

titanium grid (the silane layers face-to-face) by carbon glue. The glued grid was pre-thinned by hand and then with dimple grinder (Model 656, Gatan Inc., USA) to the thickness of ~50 μm. The final thinning was made with precision ion polishing system (PIPS, Model 691, Gatan Inc., USA).

A field emission scanning electron microscope (FESEM, Zeiss ULTRAplus, Zeiss, Germany), operated at an accelerating voltage of 15 kV, was used to study the silane layers on the various stainless steel surfaces, the prepared injection-molded steel-silane-TPU hybrid parts, and the peeled surfaces of the hybrid. Cross-sectional sample preparation for FESEM from silanized stainless steel inserts was very challenging. Conventional metallographic cross-sectional sample preparation turned out to be unsuitable for these samples because silane reacted with sample preparation resin. Bending the samples in liquid nitrogen, like described in Ref. [17], was not successful because of the silane layer did not become brittle enough. In earlier study [20], very simple sample preparation method was implemented and it was used also in this study: the silanized steel surface was glued with carbon glue on an aluminum SEM stub and with a surgical blade an incision was produced through the silane layer. From the edges of the incision, the cross-sections of the layers could be characterized by tilting (20 - 25°) the sample from the normal position in FESEM. The cross-sectional samples from the injection-molded hybrid parts were prepared by conventional metallographic sample preparation.

2.3.4. Peel test

The peel strength values of the finished insert-injection-molded hybrid parts were measured using 180 ° peel test (modification from ASTM D 903-98). Samples were conditioned before testing at 23 ± 1 °C in 50 ± 2 % relative humidity for 72 hours. A testing machine (Messphysik, Austria) with a 1 kN load cell and 100 mm/min crosshead speed was used. The test was repeated 6-10 times for each type of sample. Peeled sample surfaces were studied with FESEM and AFM.

3. RESULTS AND DISCUSSION

3.1. AFM results

The images of the silanized steel inserts are presented in Fig. 1. During drying and curing of the inserts, a thicker silane layer formed on the middle area of the insert in the transverse direction. Therefore, AFM images were taken both from the middle and from the edge areas in the transversal direction of the insert, these areas are marked with rectangles in Fig. 1. Because the silanized steel inserts were cured in the angle of 30 °, the inserts were studied with AFM also from three areas in the longitudinal direction to find out the topography of the silane layer in the upper, middle, and bottom area of the insert, marked with 1, 2, and 3, respectively, in Fig. 1. About 65 % of the steel inserts were silanized and the upper parts of the inserts had no silane. The schematic drawing, bottom-end-view, of the formed silane layer on the polished and oxidized steel surface with thicker middle area and thinner edge areas in the transverse direction of the insert is presented in Fig. 1 (d).

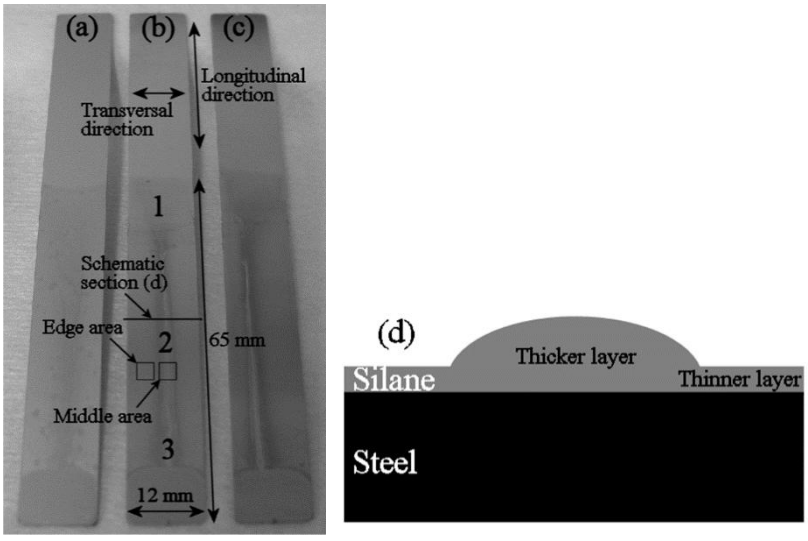

Figure 1. The images of silanized steels, (a) cleaned, industrially pickled steel insert, (b) electrolytically polished and 5 min oxidized steel insert, and (c) electrolytically polished and 100 min oxidized steel insert. Studied areas are marked with rectangles (middle and edge areas in transverse direction) and with numbers (areas in longitudinal direction). (d) Schematic drawing, bottom-end-view, of formed silane layer on polished and oxidized steel surface with thicker middle area and thinner edge areas in transverse direction of insert.

AFM images of the cleaned pickled steel surface and modified (electrolytically polished and 5 or 100 min oxidized) steel surfaces and the surfaces after silane treatment are presented in Fig. 2. The industrially pickled surface is much rougher compared to modified surfaces and therefore, the scanned area (13 μm x 13 μm, z = 2 μm) of the images of the pickled steel surface is larger than with modified surfaces (2 μm x 2 μm, z = 1 μm). On the cleaned, industrially pickled steel surface, the grain boundaries are clearly visible (Fig. 2 (a)). After electrolytical polishing, the surface is smooth (AFM image not shown) and the grain boundaries are not detected anymore. During 100 minutes oxidation, the uniform oxide layer forms on the polished stainless steel surface (Fig. 2 (c)) while 5 minutes oxidized steel surface has uneven layer (Fig. 2 (b)). After silane treatment, silane can be detected mainly in the grain boundaries of the pickled steel surface (Fig. 2 (d)). The formed silane layer was similar on the both 5 and 100 minutes oxidized steel surfaces. The topography of the silane layer on the middle area of the insert is presented in Fig. 2 (e). In the both areas, middle and edge areas, topography of the oxide layer is totally covered by silane and the top of the silane layer is smooth. Topographies of the silane layers in studied areas 1, 2, and 3 (indicated in Fig. 1) were very similar. Hence, the curing angle of 30° did not affect the formed silane layer topography in longitudinal direction of the steel inserts.

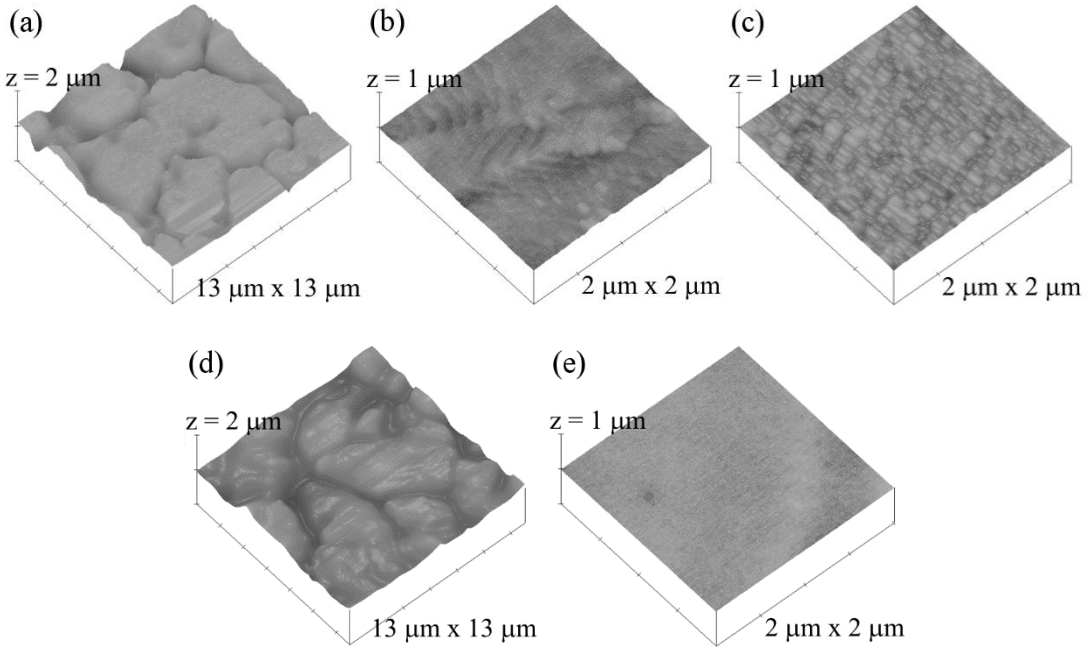

Figure 2. AFM images of (a) cleaned, industrially pickled steel, R_a is 57 nm, (b) electrolytically polished and 5 min oxidized steel, R_a is 12 nm, (c) electrolytically polished and 100 min oxidized steel, R_a is 4 nm, (d) silanized pickled steel, R_a is 56 nm, (e) polished and oxidized steel after silane treatment, middle area of insert, R_a is 0.6 nm. Notice different scales in (a) and (d) compared to (b), (c), (e), and (f).

3.2. XPS results

Samples for XPS analyses were taken from the cleaned, industrially pickled and polished, 100 min oxidized stainless steel surfaces before and after silanization. Moreover, samples of both thin and thick silane layers on the 100 min oxidized surface (edge and middle areas indicated in Fig. 1, respectively) were analyzed. The information depth was ~8 nm from the outermost surface (three times the inelastic mean free path value of photoelectrons in silane materials) [8].

XPS survey spectra indicating the elements present on the steel surfaces before silanization are shown in Fig. 3 (a), while narrow scan spectra and identification of chemical states from C 1*s* and O 1*s* transitions are shown in Figs. 3 (b) and (c) respectively. The C 1*s* spectra were fitted with two components (C–C at 285.2 eV and C=O at 288 eV), whereas three components were used for O 1*s* (M–O at 530.2 eV, –OH at 531.9 eV, and C=O at 533 eV). Relative concentrations of the chemical species (in atomic-%) are presented in Table 2. According to the analysis results, the cleaned,

pickled surface consisted of the stainless steel alloy (XPS contributions from metallic Fe and Cr) and a thin surface oxide film (Fe and Cr oxides and hydroxides) that were largely covered by carbonous impurities (organic compounds containing C–C and C=O type bonds). Ca, N, and F due to the pickling process were detected as trace elements near the detection limit of XPS (~0.1 at.%). The surface oxide was representative of a typical passive layer on stainless steel, i.e., it was enriched with Cr oxides but contained no Ni, and approximately 1-3 nm thick [21]. Polishing and subsequent 100 min oxidation of the material, however, produced a thick oxide layer consisting of mainly Fe_2O_3 at the outermost surface, as indicated by the Fe 2p peak at 711.2 eV corresponding purely to Fe3+ species (not shown). In addition, the amount of C from surface impurities was reduced considerably from 59.6 at.% to 17.4 at.% as a result of the treatment. Mn, Ca, P, and Zn were detected as trace elements on the polished and oxidized surface.

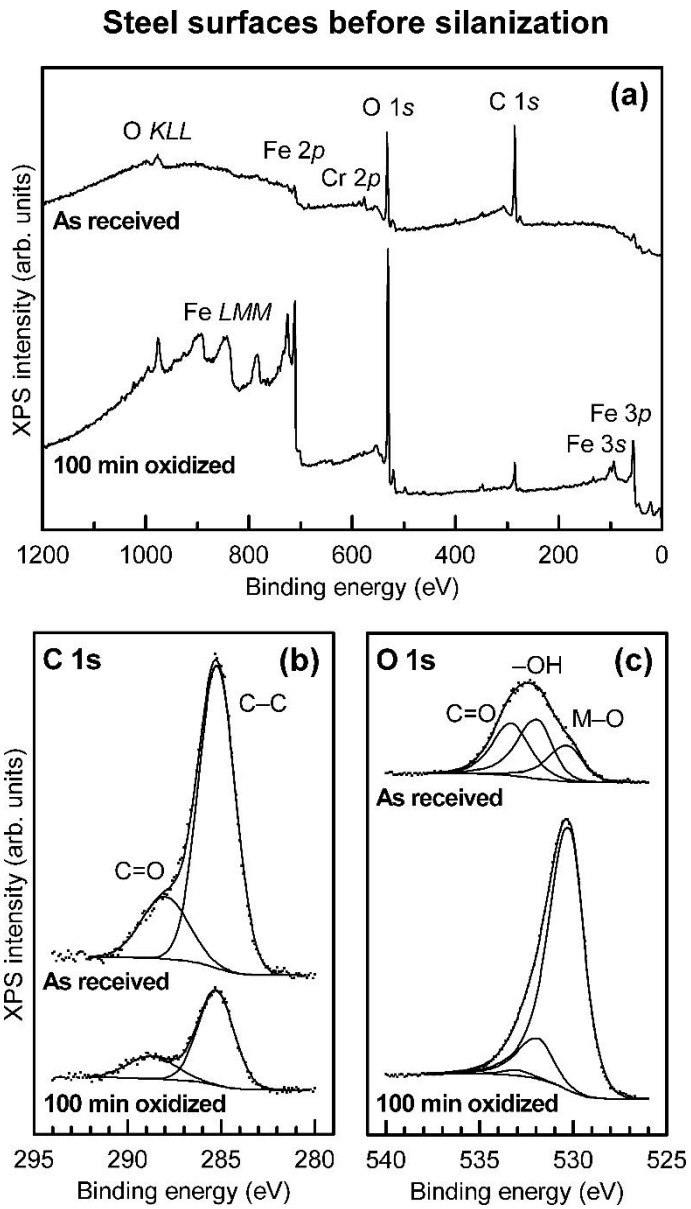

Figure 3. (a) XPS survey spectra, (b) C 1*s* spectra, and (c) O 1*s* spectra obtained from cleaned, industrially pickled and 100 min oxidized stainless steel surfaces before silanization.

Table 2. Relative concentrations of chemical species (in atomic-%) on the cleaned, industrially pickled stainless steel surface and polished, 100 min oxidized stainless steel surfaces before silanization as determined by XPS. The bulk composition of AISI 304 stainless steel is included for reference.

	Relative concentration (at%)									
	Fe (met)	Fe (ox.)	Cr (met)	Cr (ox.)	Ni (met)	C (C–C)	C (C=O)	O (M–O)	O (–OH)	O (C=O)
Bulk alloy	73.0		19.2		7.6					
Surface, as-received	0.6	1.7	0.2	1.9	-	47.2	12.4	8.7	14.3	13.1
Surface, el. polished +100 min oxidized	-	12.9	-	0.4	-	13.2	4.2	59.4	9.1	0.9

A schematic representation of surface morphology of the cleaned, industrially pickled and 100 min oxidized stainless steel surfaces before silanization is shown in Fig. 4. The carbonous impurities were probably due to organic compounds originating from the atmosphere or packing materials of the as-received steel plates and so they could not be totally removed with ethanol and acetone cleaning in the ultrasonic cleaner which was carried out for the as-received samples. Both surfaces contained an appreciable amount of hydroxyl species resulting from reactions with ambient water, which is required for the efficient bonding of silanes.

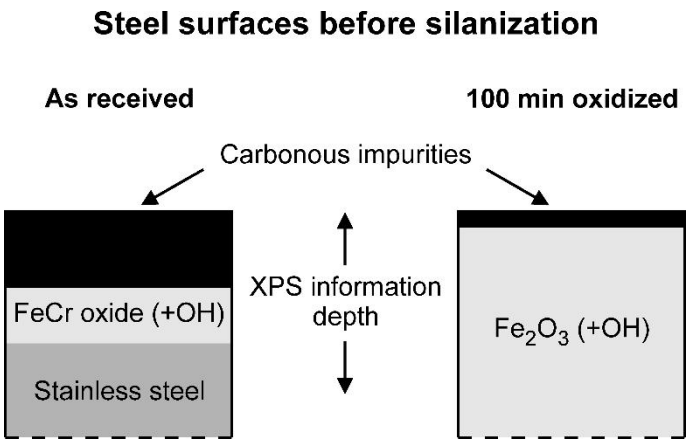

Figure 4. Schematic representation of surface morphology (cross-section of the layer structure) of cleaned, industrially pickled and polished, 100 min oxidized stainless steel surfaces before silanization.

In order to determine the chemical composition of the produced silane layers and to evaluate their quality in this respect, further XPS analyses were carried out after silanization. Survey spectra obtained from the surfaces after silanization are shown in Fig. 5 (a), while narrow scan spectra of the C 1*s* and O 1*s* transitions are shown in Figs. 5 (b) and (c), respectively. Relative concentrations of chemical species (in atomic-%) are presented in Table 3. The results were consistent with the formation of g-AEAPS silane layers on top of stainless steel, indicated by the appearance of Si 2*p* (103.2 eV) and N 1*s* (400.6 eV) signals from the silane as well as attenuation of the Fe 2*p* and O 1*s* (M–O) signals from the substrate, with less attenuation in the case of a thin silane layer. The N 1*s* peak position was characteristic of amino type species (e.g. $–NH_2$), indicating no reaction of the aminofunctional groups during the preparation of the layer. The C 1*s* (C–C) signal originating from silanes was shifted towards higher binding energies (up to 286.3 eV) in comparison to that from carbonous impurities. In addition, the O 1*s* component related to siloxane bonds (Si–O–Si, at 533.1 eV) increased in intensity. However, this component still included some contribution from C=O type species due to atmospheric impurities (CO_2, CH_2O, etc.) [22], as indicated by the C 1*s* spectra (the component at 288 eV). No further impurities apart from those originally present on the stainless steel surfaces were detected.

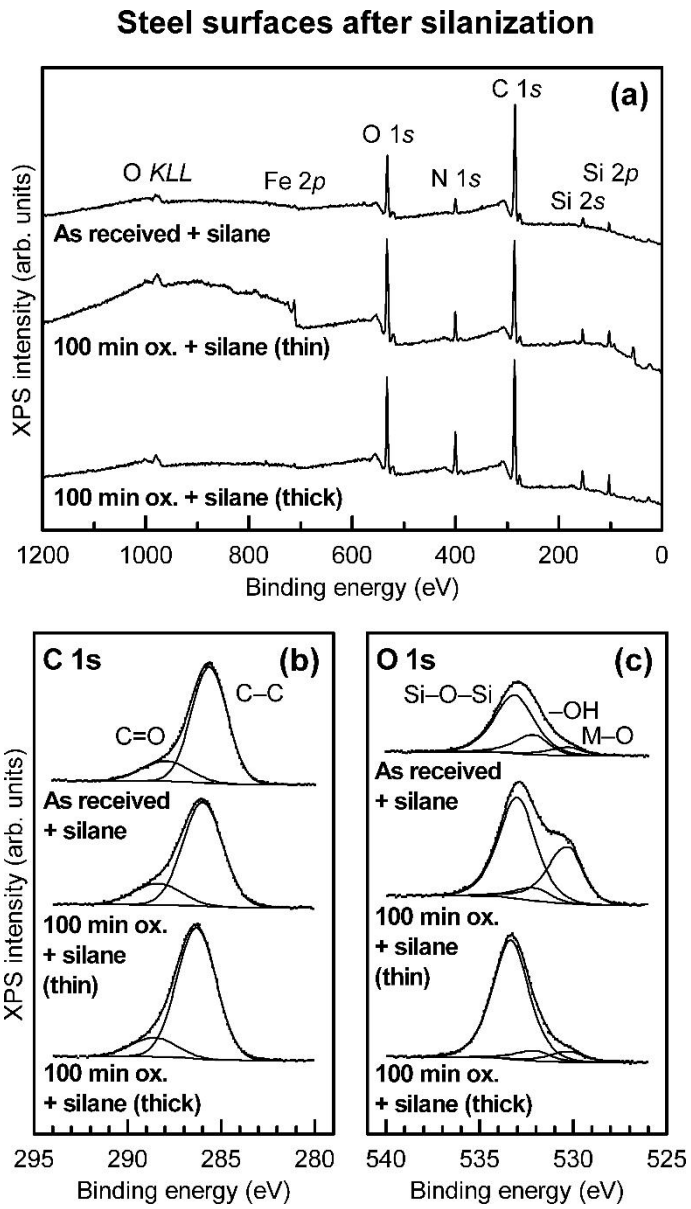

Figure 5. (a) XPS survey spectra, (b) C 1*s* spectra, and (c) O 1*s* spectra obtained from cleaned, industrially pickled stainless steel surface and polished, 100 min oxidized stainless steel surfaces after silanization. In the case of 100 min oxidized surface, spectra corresponding to thin silane layer at edge of insert and to thick silane layer in middle of insert are shown.

Table 3. Relative concentrations of chemical species (in atomic-%) on as-received and 100 min oxidized stainless steel surfaces after silanization as determined by XPS. Ideal composition of fully hydrolyzed and condensed g-AEAPS polymer is included for reference. Calculated ratio of C to Si is also indicated.

	Relative concentration (at%)									
	Fe (ox.)	Cr (ox.)	C (C–C)	C (C=O)	O (M–O)	O (–OH)	O (Si–O–Si)	N	Si	C/Si ratio
g-AEAPS			52.6				15.8	21.1	10.5	5.0
Pickled + silane	0.3	0.4	54.7	12.7	1.9	4.5	15.1	5.4	4.8	14.0
El. polished +100 min oxidized + silane (thin)	1.9	-	40.6	10.0	10.1	2.3	18.4	10.0	6.7	7.5
El. polished + 100 min oxidized + silane (thick)	0.3	-	49.3	8.2	1.7	1.7	20.5	9.9	8.4	6.9

The main differences between the silanized industrially pickled surface and 100 min oxidized surfaces were apparent from the relative concentrations given in Table 3. Firstly, the silane coverage obtained on the pickled surface was considerably less than on the oxidized surface, as seen from the relative concentrations of Si. On the other hand, the C/Si ratio was very high on the silanized pickled surface, indicating that the surface was still largely covered by carbonous impurities, whereas on the 100 min oxidized surface the ratio was closer to the value of pure g-AEAPS polymer. Thus, the presence of impurities on the pickled surface seemed to hinder the formation of a uniform silane layer, but this issue was remedied by the polishing and oxidation pre-treatment. Concerning subsequent utilization of the silanized surfaces, the amount of N (amino) species needed for the bonding of TPU or similar materials was also favorable on the 100 min oxidized surface.

3.3. TEM and SEM results

3.3.1. Silane layer on steel inserts after silane treatment

TEM samples were prepared by scraping the silane layer from the silanized inserts on the carbon grid to determine the composition of the silane layer. TEM images, selected area electron diffraction (SAED) patterns, and EDS analyses were very similar between various areas of the insert (Fig. 1) and also between various steel surfaces. TEM image and SAED pattern of the scraped silane on the 100 minutes oxidized steel surface are presented in Fig. 6. The structure of the layer is very uniform and the SAED pattern shows the amorphous character of the silane layer. The EDS results were: 13 at.% Si, 75 at.% C, and 9 at.% O (+ e.g. Ca, Cl, P). The calculated C/Si-ratio is 5.8, which is close to that ratio calculated from XPS results (Tab. 3). Despite of the strong film-substrate adhesion, no changes in the properties of the silane layer were observed with TEM due to sample preparation. Because of the silane layer seemed similar from both top-view and cross-sectional-view samples (e.g. the composition and SAED pattern).

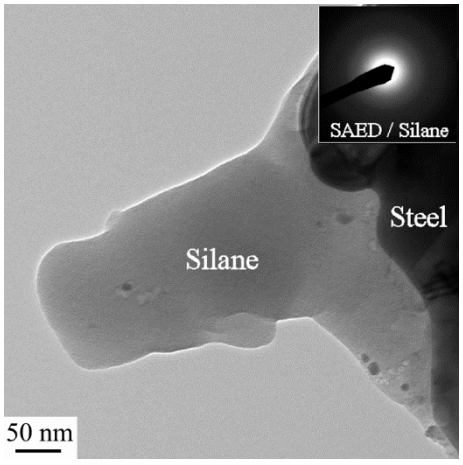

Figure 6. TEM image and SAED pattern of scraped silane.

FESEM and TEM images (cross-sectional) of the silane layer on electrolytically polished and 100 min oxidized steel insert are presented in Fig. 7. The images are from the area 2 (indicated in Fig. 1) because all three areas in longitudinal direction of the inserts were very similar. This indicates that the curing angle of 30° did not affect the silane layer thickness in the longitudinal direction. However, thickness varied between the middle area and the edge areas of the inserts in the transverse direction. According to FESEM and TEM results, the silane layer thickness is very different between the middle area with thickness of 150 nm (Figs. 7 (a) and (b)) and the edge areas with thickness of 20 nm (Figs. 7 (c) and (d)). FESEM results about layer thickness were comparable to TEM results. According to FESEM and TEM studies, the silane layers were very similar on the both 5 and 100 minutes oxidized steel surfaces. On the pickled steel surface, the silane layer thickness varied much between grains and grain boundaries. In the grain boundaries, the layer thickness was around 100 nm while the layer was very thin on the grains. The situation was similar through the whole insert and differences between the middle and edge areas were not detected with the pickled insert. The silane layer seemed to be even on all steel surfaces in longitudinal direction but the thickness varies more on the pickled surface due to grain boundaries while with polished and oxidized steel inserts, the silane layer thickness varies only between the middle area and the edge areas in the transverse direction but inside these areas, the layer thickness was very even.

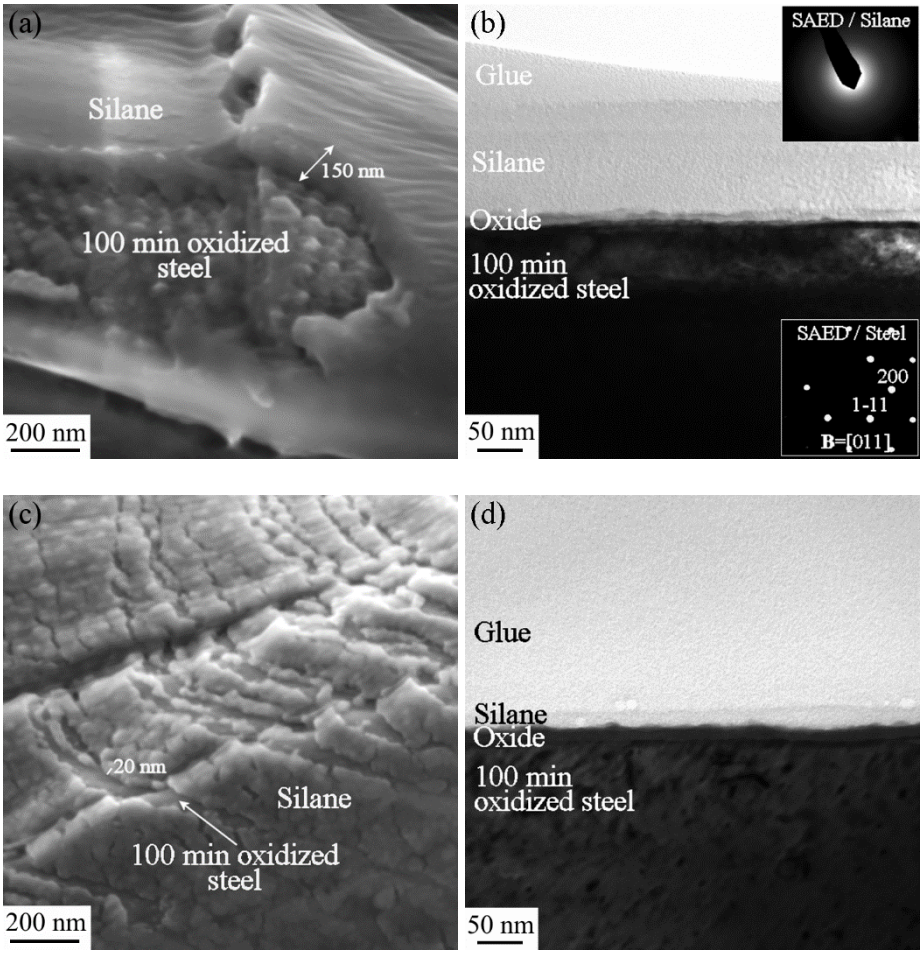

Figure 7. FESEM and TEM images of silane layer on electrolytically polished and 100 min oxidized steel surface. (a) FESEM and (b) TEM image of middle area of insert in transverse direction with thick silane layer (150 nm), (c) FESEM and (d) TEM image of edge area in transverse direction with thin silane layer (20 nm).

3.3.2. Silane layer on steel insert after injection molding

Cross-sectional FESEM samples of the injection-molded hybrids, to find out the effects of the injection molding on the silane layer, were prepared from same areas 1, 2, and 3 (indicated in Fig. 1) like after the silane treatment. The sample preparation was very challenging and for example in the case of the hybrid with the pickled steel insert, TPU easily detached from the steel surface. Cross-sections of the steel-TPU hybrids with modified steel inserts were very similar and no differences between areas 1-3 were detected. Cross-sectional FESEM image of the steel-TPU hybrid with polished and 100 min oxidized steel insert from the middle area of the insert in both

transverse and longitudinal directions is presented in Fig. 8. In the middle area, the silane layer thickness is around 200 nm and its bonding to the steel surface is good without any cracks or pores.

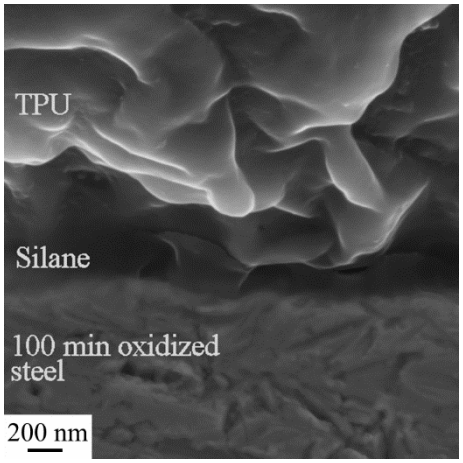

Figure 8. Cross-sectional FESEM image of steel-TPU hybrid with polished and 100 min oxidized steel insert (middle area of insert in transverse and longitudinal directions).

3.4. Peel results

Peel strengths with standard deviations of the steel-TPU hybrids with various steel inserts, cleaned pickled, electrolytically polished and 5 or 100 min oxidized, were 82 ± 12 N/cm, 166 ± 4 N/cm, and 166 ± 8 N/cm, respectively. In practice, with 100 min oxidized insert, the peel value was even better because the TPU part of two hybrids out of six broke cohesively during peel test. The images of the steel inserts after peel test are presented in Fig. 9, modified steel inserts are covered by TPU except the middle area of the insert with thick silane layer (Fig. 9 (b) and (c)) but the pickled insert has no TPU on it (Fig. 9 (a)). Peeled samples were studied with FESEM and AFM. Summary of FESEM and AFM images is presented in Table 4.

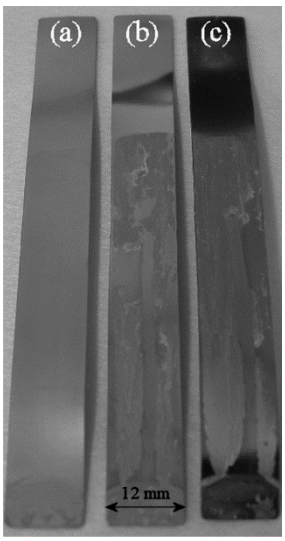

Figure 9. Images of steel inserts after peel test. (a) Cleaned, pickled steel insert, (b) electrolytically polished and 5 min oxidized steel insert, and (c) electrolytically polished and 100 min oxidized steel insert.

Table 4. Summary of FESEM and AFM images of peeled surfaces.

Insert used in peeled hybrid		FESEM	AFM
Cleaned, industrially	Steel side	Fig. 13 (a)	-
pickled	TPU side	Fig. 13 (b)	-
Elect. polished +	Steel side	Fig. 10 (a) and (b)	Fig. 10 (c)
5 min oxidized	TPU side	Fig. 11	-
Elect. polished +	Steel side	Fig. 12 (a) and (b)	-
100 min oxidized	TPU side	-	-

According to FESEM studies of the peeled hybrids manufactured using 5 or 100 minutes oxidized steel inserts, failure types were very similar. Various failure types, cohesive in TPU, adhesive in silane/TPU interface and cohesive in silane layer, were detected. FESEM and AFM images of the peeled steel side (5 min oxidized) from the middle area of the insert in the transverse direction with thicker silane layer are presented in Fig. 10. In that area, few TPU islands are visible on the steel side showing cohesive failure in TPU (T/T in Fig. 10 (a)). The failure also exists as adhesive in silane/TPU interface (S/T in Fig. 10 (a), (b), and (c)) which occurs as a network structure. In that area, the top of the silane layer (Fig. 10 (c)) is as smooth as after silane treatment (Fig. 2 (c)) indicating that its bonding with TPU has been poor. However, in the thick silane layer area, the failure mainly exists in the silane layer (S/S in Figs. 10 (a) and (b)). It can be assumed from the AFM studies, showing that the electrolytically polished and 5 minutes oxidized steel surface

without silane layer (Fig. 2 (a)) has not surface structure as in Fig. 10 (b) and (c) so the failure does not happen in the steel/silane interface but inside the silane layer. Replica structures for the steel side can be detected in the TPU side as presented in Fig. 11. In the silane/silane failure areas, the most of the silane layer thickness is in TPU side indicating that silane/silane cohesive failure happens very close to the steel surface.

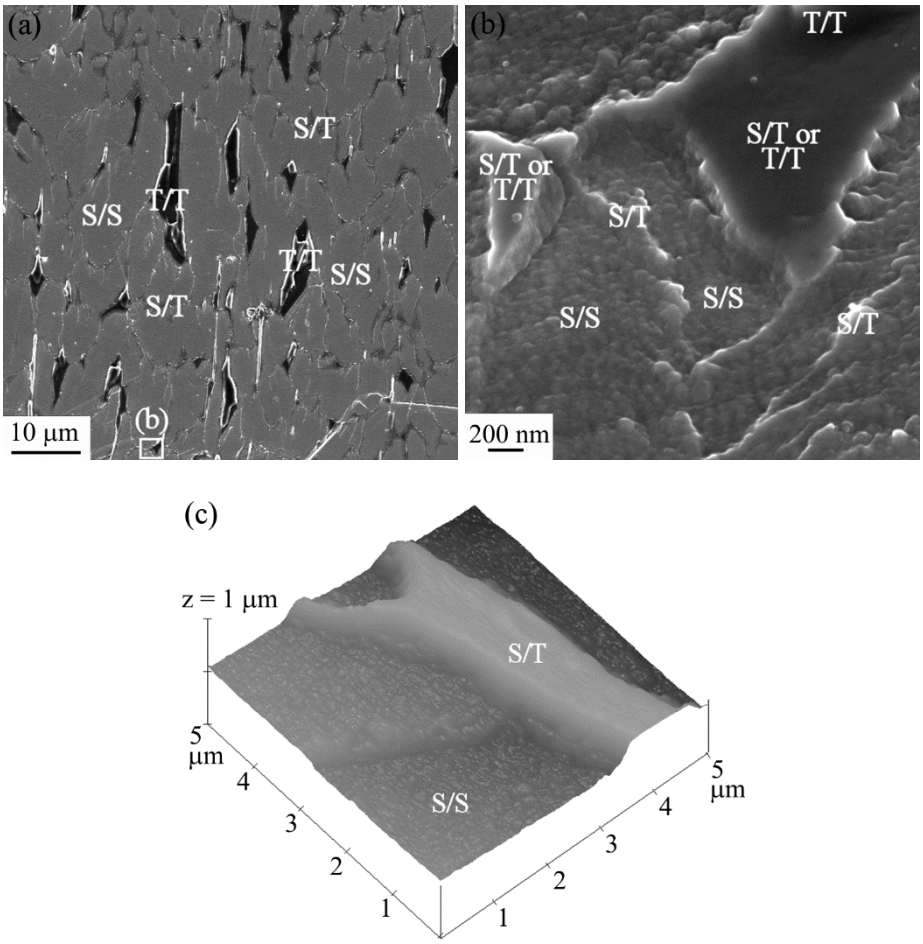

Figure 10. Peeled surfaces, steel side, of injection-molded hybrid with electrolytically polished and 5 min oxidized insert with thick silane layer. (a) And (b) FESEM images and (c) AFM image. S/S is failure in silane layer, S/T is adhesive failure in silane/TPU interface, and T/T is cohesive failure in TPU.

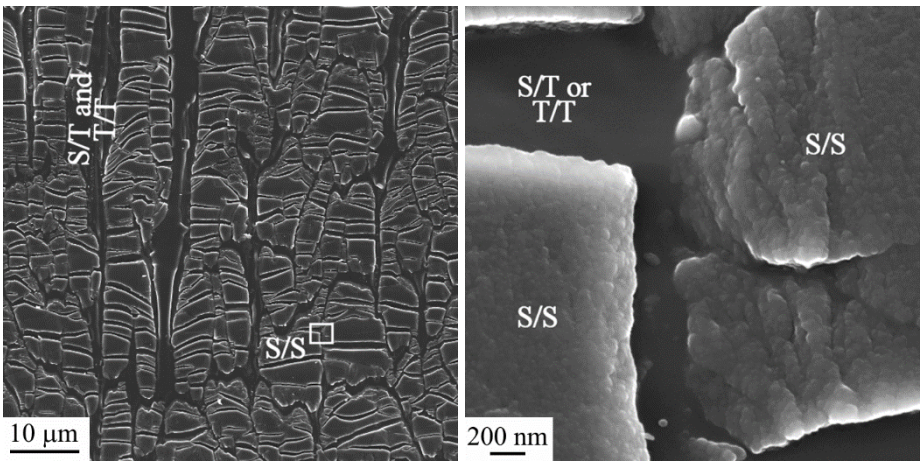

Figure 11. FESEM images of peeled surface, TPU side, of injection-molded hybrid with electrolytically polished and 5 min oxidized insert with thick silane layer. S/S is failure in silane layer, S/T is adhesive failure in silane-TPU interface, and T/T is cohesive failure in TPU.

The steel side (electrolytically polished and 100 min oxidized) from the area with thinner silane layer is presented in Fig. 12 (a) where the failure is totally cohesive in TPU. The steel side from the boundary area between the thin and thick silane layer is presented in Fig. 12 (b) where the failure type changes from failure inside the silane layer or adhesive failure in silane/TPU interface (with thick silane layer) to totally cohesive failure in TPU (with thin silane layer).

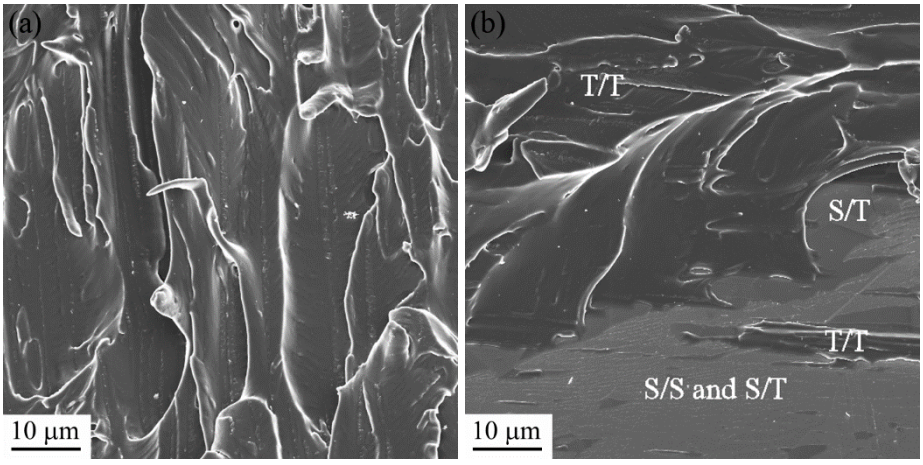

Figure 12. FESEM images of peeled surfaces, steel side, of injection-molded hybrid with electrolytically polished and 100 min oxidized steel from (a) area with thin silane layer and (b) boundary area between thin (top of image) and thick (bottom of image) silane layer. S/S is failure in silane layer, S/T is adhesive failure in silane-TPU interface, and T/T is cohesive failure in TPU.

After the peel test, the hybrid with industrially pickled steel insert has no differences between middle area and edge areas in the transverse direction as can be seen from Fig. 9 (a). FESEM images of pickled steel side and TPU side are presented in Figs. 13 (a) and (b), respectively. The failure inside the silane layer dominates. In the grain boundaries, the silane layer is thicker remaining on the both steel and TPU sides. With the cleaned, pickled steel insert, cohesive failure in TPU was not detected which was expected because of the peel strength was low compared to the strengths of the hybrids with polished and oxidized inserts. According to XPS results, the amount of the carbonous impurities (Tab. 3) was significant on silanized pickled steel which may disturb the well-bonded silane layer formation. In addition, the amount of N (amino) species was less on the silane layer surface of pickled steel than that of on polished and 100 min oxidized steel (Tab. 3). Probably, this caused poor bonding between pickled steel and TPU resulting low peel strength and no observable cohesive failure in TPU but adhesive failure in the silane-TPU interface.

As a conclusion of the peel test results, the steel surface structure prior to silanization and the formed silane layer thickness affected significantly the peel strength of the steel-TPU hybrids. The hybrids manufactured using the steel insert with a controlled oxide layer had significantly better peel strength compared to the hybrid with the pickled steel insert or according to previous study [1] with the electrolytically polished steel insert without a controlled oxide layer. Therefore, also a controlled oxide layer is needed in addition of a clean and smooth surface to achieve good bonding between silane and steel. Also the rough surface of pickled steel can disturb the well-bonded silane layer formation [4]. According to XPS results, cleaned, pickled steel also had more carbonous impurities on the surface compared to the polished and oxidized steel surface, which may disturb the silane bonding on the steel surface. To verify this, for example, infrared spectroscopy can be used to study bonds in the silane/steel interfaces. In addition, the surface of the silane layer on pickled steel had less N (amino) species to react with TPU than that of on oxidized steel resulting probably poor silane bonding to TPU. According to FESEM images of the peeled surfaces, the optimal silane layer thickness would be around 20 nm because of cohesive failure in TPU occurred

in the areas with that thickness with polished and oxidized steel inserts. While with thicker layer (around 150 nm), the failure existed mainly inside the silane layer. This agrees with Li's *et al.* [10] studies that a thick silane layer can contain weak interface layers which decrease adhesive strength. According also to earlier study [9], too thin or thick layer decreases adhesive strength. In that study [9], with around 10 nm thick silane layer (from the solution concentration of 0.1 vol%), peel strengths decreased around 40 % and with 100-300 nm thick silane layer (from the solution concentration of 1 vol%) around 30 % compared to peel strengths in this study [9].

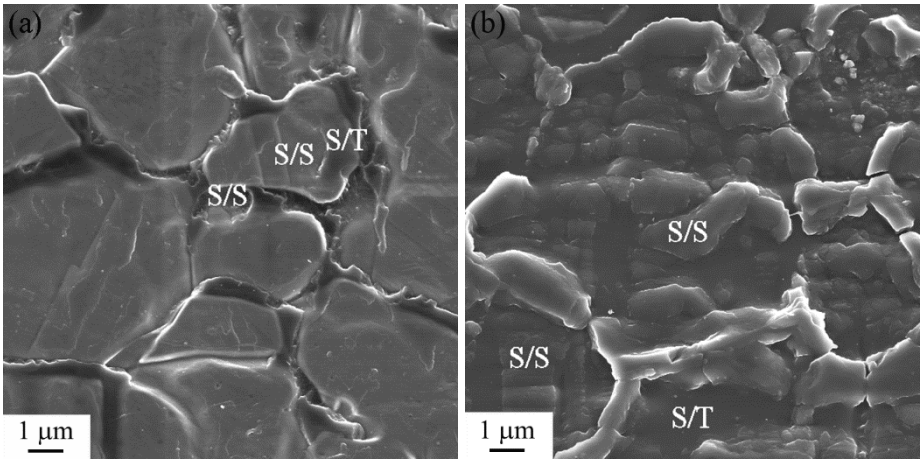

Figure 13. FESEM images of peeled surfaces of injection-molded hybrid with pickled steel. (a) steel side and (b) TPU side. S/S is failure in silane layer, S/T is adhesive failure in silane-TPU interface, and T/T is cohesive failure in TPU.

4. CONCLUSIONS

The aim of this study was to comprehensively characterize silane layers on the modified stainless steel surfaces and relate it to the adhesion in the stainless steel-TPU hybrids. According to the previous study [1], the stainless steel-TPU hybrid structures could be manufactured with injection molding process. In addition, initial results of the effect of the stainless steel surfaces on the adhesion strength of the hybrids were achieved [1]. However, the detailed characterization of the silane layers was lacking and so it was carried out in this study. Prior to silane treatment, modification (electrolytical polishing and oxidation treatment in air at 350°C for 5 or 100 min) of

the steel inserts was used to achieve better silane bonding to the steel surface. In the cleaned, industrially pickled steel surface, silane existed mainly in the grain boundaries. The hybrids, manufactured with pickled steel inserts, failed mainly inside the silane layer and no cohesive fail in TPU was detected. While, the hybrids, manufactured with surface-modified steel insert, had more uniform silane layer and they failed mainly cohesively in TPU resulting better peel strength compared to the hybrid with pickled steel insert. XPS results indicated that the formation of a uniform silane layer was hindered by carbonous impurities on the pickled surface, whereas polishing and oxidation treatment produced a clean Fe_2O_3-type surface oxide with improved bonding properties. In addition, the formed silane layer surface on cleaned, industrially pickled steel had less N (amino) species to react with TPU compared to the silane layer on the modified steel surface. During silanization, two different areas in the transverse direction of the insert formed on the polished and oxidized steel surfaces: the middle area of the insert with a thick silane layer (150 nm) and the edge areas with a thin silane layer (20 nm). The areas with thick silane layers failed mainly inside the silane layer and with the thin silane layers cohesively in TPU. So, the polished and oxidized steel surface and the relatively uniform, around 20 nm thick, silane layer are needed to achieve well-bonded stainless steel-TPU hybrids. AFM, FESEM, and TEM studies of the silane layer during manufacturing and testing steps of the hybrids proved to be very useful to get information about silane layer and failure types. In order to get these hybrids for real applications, further studies about long-term stability tests should be carried out.

Acknowledgements

The authors thank Graduate School of Processing of Polymers and Polymer-based Multimaterials, Finnish Funding Agency for Technology and Innovation (TEKES, grant Nos. 230007, 210031, and 230053), The Academy of Finland (grant No. 320019), The National Graduate School in Materials Physics, Technology Industries of Finland Centennial Foundation, and Finnish industry for financial support.

References:

[1] M. Honkanen, M. Hoikkanen, M. Vippola, J. Vuorinen, T. Lepistö, Metal-Plastic Adhesion in Injection-Molded Hybrids, J. Adhes. Sci. Technol. 23 (2009) 17471761.

[2] G. Pritchard, Coupling agents, in: G. Pritchard (Ed.) Plastic Additives, Chapman & Hall, London, 1998, pp. 189-196.

[3] E. Plueddemann, Silane coupling agents, Plenum Press, New York, 1982.

[4] Primers and adhesion promoters, in: E. Petrie (Ed.), Handbook of Adhesives and Sealants, McGraw-Hill, New York, 2007, pp. 277-305.

[5] T. Van Schaftinghen, C. Le Pen, H. Terryn, F. Hörzenberger, Investigation of the barrier properties of silanes on cold rolled steel, Electrochim. Acta 49 (2004) 2997-3004.

[6] W. van Ooij, D. Zhu, M. Stacy, A. Seth, T. Mugada, J. Gandhi, P. Puomi, Corrosion Protection Properties of Organofunctional Silanes – An Overviw, Tsinghua Science and Technology 10 (2005) 639-664.

[7] V. Palanivel, D. Zhu, W. van Ooij, Nanoparticle-filled silane films as chromate replacements for aluminum alloys, Prog. Org. Coat. 47 (2003) 384-392.

[8] P. Jussila, H. Ali-Löytty, K. Lahtonen, M. Hirsimäki, M. Valden, Effect of surface hydroxyl concentration on the bonding and morphology of aminopropylsilane thin films on austenitic stainless steel, Surf. Interface Anal. 42 (2010) 157-164.

[9] M. Hoikkanen, M. Honkanen, M. Vippola, T. Lepistö, J. Vuorinen, Effect of Silane Treatment parameters on the Silane layer Formation and Bonding to Thermoplastic Urethane, submitted to Prog. Org. Coat.

[10] G. Li, X. Wang, A. Li, W. Wang, L. Zheng, Fabrication and adhesive properties of thin organosilane films coated on low carbon steel substrates, Surf. Coat. Technol. 201 (2007) 9571-9578.

[11] M. Honkanen, M. Vippola, T. Lepistö, Characterisation of Stainless Steel Surfaces – Modified in air at 350 °C, Surf. Eng., DOI 10.1179/174329409X397750.

[12] D. Susac, X. Sun, K. Mitchell, Adsorption of BTSE and g-APS organosilanes on different microstructural regions of 2024-T3 aluminum alloy, Appl. Surf. Sci. 207 (2003) 40-50.

[13] J. Kim, P. Wong, K. Wong, R. Sodhi, K. Mitchell, Adsorption of BTSE and g-GPS organosilanes on different microstructural regions of 7075-T6 aluminum alloy, Appl. Surf. Sci. 253 (2007) 3133-3143.

[14] W. Yuan, W. van Ooij, Characterization of Organofunctional Silane Films on Zinc Substrates, J. Colloid Interf. Sci. 185 (1997) 197-209.

[15] C. Le Pen, B. Vuillemin, S. Van Gils, H. Terryn, R. Oltra, In-situ characterization of organosilane film formation on aluminium alloys by electrochemical quartz crystal microbalance and in-situ ellipsometry, Thin Solid Films 483 (2005) 66-73.

[16] A. Franquet, J. De Laet, T. Schram, H. Terryn, V. Subramanian, W. Van Ooij, J. Vereecken, Determination of the thickness of thin silane films on aluminium surfaces by means of spectroscopic ellipsometry, Thin Solid Films 384 (2001) 37-45.

[17] I. De Graeve, E. Tourwé, M. Biesemand, R. Willem, H. Terryn, Silane solution stability and film morphology of water-based bis-1,2-(triethoxysilyl)ethane for thin-film deposition on aluminium, Prog. Org. Coat. 63 (2008) 38-42.

[18] N. Fairley, *CasaXPS: Spectrum Processing Software for XPS, AES and SIMS (Version 2.3.13)*, Casa Software Ltd, Cheshire, 2006, http://www.casaxps.com/.

[19] C.D. Wagner, A.V. Naumkin, A. Kraut-Vass, J.W. Allison, C.J. Powell, J.R. Rumble Jr., *NIST XPS Database, Version 3.5 (Web Version)*, National Institute of Standards and Technology, 2007, http://srdata.nist.gov/xps/.

[20] M. Honkanen, M. Hoikkanen, M. Vippola, J. Vuorinen, T. Lepistö, Electron microscopy of Silane Layers in Stainless Steel – TPU Hybrids, in: Proceedings of 61st Annual Meeting of the Scandinavian Society for Electron Microscopy, Stockholm, Sweden, June 8-10, 2010.

[21] C.-O.A. Olsson, D. Landolt, Passive films on stainless steels – chemistry, structure and growth, Electrochim. Acta 48 (2003) 1093-1104.

[22] H.L. Cabibil, V. Pham, J. Lozano, H. Celio, R.M. Winter, J.M. White, Self-Organized Fibrous Nanostructures on Poly[(aminopropyl)siloxane] Films Studied by Atomic Force Microscopy, Langmuir 16 (2000) 10471-10481.